

Lamellar fluctuations melt ferroelectricity

G. G. Guzmán-Verri^a

Centro de Investigación en Ciencia e Ingeniería de Materiales,

Universidad de Costa Rica, San José, Costa Rica 11501,

Escuela de Física, Universidad de Costa Rica, San José, Costa Rica 11501, and

Department of Materials Science and Metallurgy,

University of Cambridge, Cambridge, UK CB3 0DS.

C. H. Liang

James Franck Institute, University of Chicago, Chicago, Illinois, USA 60637, and

Pritzker School of Molecular Engineering,

University of Chicago, Chicago, Illinois, USA 60637.

P. B. Littlewood^b

James Franck Institute, University of Chicago, Chicago, Illinois, USA 60637.

(Dated: April 26, 2023)

arXiv:2205.14171v3 [cond-mat.mtrl-sci] 25 Apr 2023

^a gian.guzman@ucr.ac.cr

^b littlewood@uchicago.edu

Abstract

We consider a standard Ginzburg-Landau model of a ferroelectric whose electrical polarization is coupled to gradients of elastic strain [1–4]. At the harmonic level, such flexoelectric interaction is known to hybridize acoustic and optic phonon modes and lead to phases with modulated lattice structures that precede the symmetry broken state for sufficiently large couplings [5–10]. Here, we use the self-consistent phonon approximation to calculate the effects of thermal and quantum polarization fluctuations on the bare modes to show that such long-range modulated order is unstable at all temperatures. We discuss the implications for the nearly ferroelectric SrTiO₃ and KTaO₃, and propose that these systems are melted versions of an underlying modulated state which is dominated by non-zero momentum thermal fluctuations except at the very lowest temperatures.

A ferroelectric (FE) material is defined by spontaneously broken inversion symmetry, usually due to a small and coherent displacement of atoms within the unit cell and hence a spontaneous electrical polarization \mathbf{P} [11]. Because lattice displacements generate the order, the homogeneity of the polarization depends on coupling between neighboring unit cells, and over longer distances by a continuous elastic strain ϵ . In a cubic (or other high symmetry FE) the principal order parameter (OP) \mathbf{P} belongs to a different irreducible representation from the strain fields ϵ at zero wavevector ($\mathbf{q} = 0$). This means that the leading order electrostrictive coupling in a uniform Landau theory for the free energy is bilinear in polarization and linear in strain (i.e. $\mathcal{O}(\epsilon P^2)$). However, also there will be in general a *flexoelectric* coupling [1–4] (i.e. $\mathcal{O}(P\nabla\epsilon)$), and it is well known that such couplings may give rise to modulated incommensurate phases within a harmonic theory, provided that the coupling is big enough [5–10]. Note that the flexoelectric coupling - being harmonic - is in principle more relevant than the nonlinear electrostrictive coupling; flexoelectricity will be the focus of this paper.

The materials SrTiO₃ (STO) and KTaO₃ (KTO) have long been cited as examples of quantum paraelectrics (QPEs). In both cases the dielectric constant follows a Curie-Weiss (CW) law divergence with a finite-temperature intercept, yet at low temperatures saturates at extremely large values [12] and there is no FE phase transition. The idea of quantum tunnelling of domains that in a mean-field like (and massive) system have already grown to be very large before quantum effects take over is disconcerting and has, over the years, generated considerable interest in the general theory of a FE quantum critical point [13–21].

Recent experiments, however, have revealed phase diagrams and lattice dynamics in STO and KTO which cannot be explained with our current understanding of these materials [22]. Specifically, high precision measurements of the dielectric response have found several crossovers (specially seen under pressure) [23–26], and, very significantly, inelastic neutron scattering experiments observe softening of a transverse acoustic (TA) mode at a small but finite wavevector in STO ($\simeq 0.025$ rlu) [27] and at a larger one in KTO ($\simeq 0.1$ rlu) [6]. The latter results are consistent with momentum-resolved electron energy-loss spectroscopy [28] and a previous neutron scattering study [29] which show an unusual softening of the TA branch, and with a first-principle simulation [30] which found a dip in the acoustic dispersion.

Soft acoustic phonons with a minimum at a finite wavevector are characteristic of systems approaching a structural instability corresponding to the onset of a long-wavelength modulation [31, 32], and can be understood as the consequence of level-repelling hybrid modes associated with a sufficiently large coupling between a primary OP (e.g. polarization) and gradients of a secondary OP (e.g. strain) [33]. However, harmonic and mean-field solutions of such models [5–10] predict the condensation of the low energy branch at a finite wavevector \mathbf{q}_{mod} , thus leading to a modulated phase which is not observed in STO and KTO. Nor can these solutions generate crossovers.

In this letter, we invoke a well-known model of flexoelectricity [1–4] and, crucially, solve it within the self-consistent phonon approximation (SCPA) in order to account for thermal and quantum fluctuations of polarization of the disordered phase. We show that in the presence of purely thermal fluctuations, the phase space for orientational fluctuations is large enough that the modulated transition is suppressed to zero temperature, and that by including zero-point quantum fluctuations, the correlation length will remain finite even at absolute zero. We estimate the parameters in comparison to KTO and STO, and find reasonable agreement with a model where the flexo-electric coupling is close to the classical critical value for the onset of a modulated phase. Our analysis suggests that the putative QPE phase of STO and KTO is largely explained by classical thermal modulated fluctuations, and that there is a second crossover to a regime dominated by quantum fluctuations at much lower temperature. However, the quantum regime in our theory does not require macroscopic quantum tunnelling, and instead arises more trivially due to zero-point occupation of orientational zero-modes. In the light of these results, we propose that STO and KTO are incipient modulated dielectrics with incommensurate order caused by the coupling of

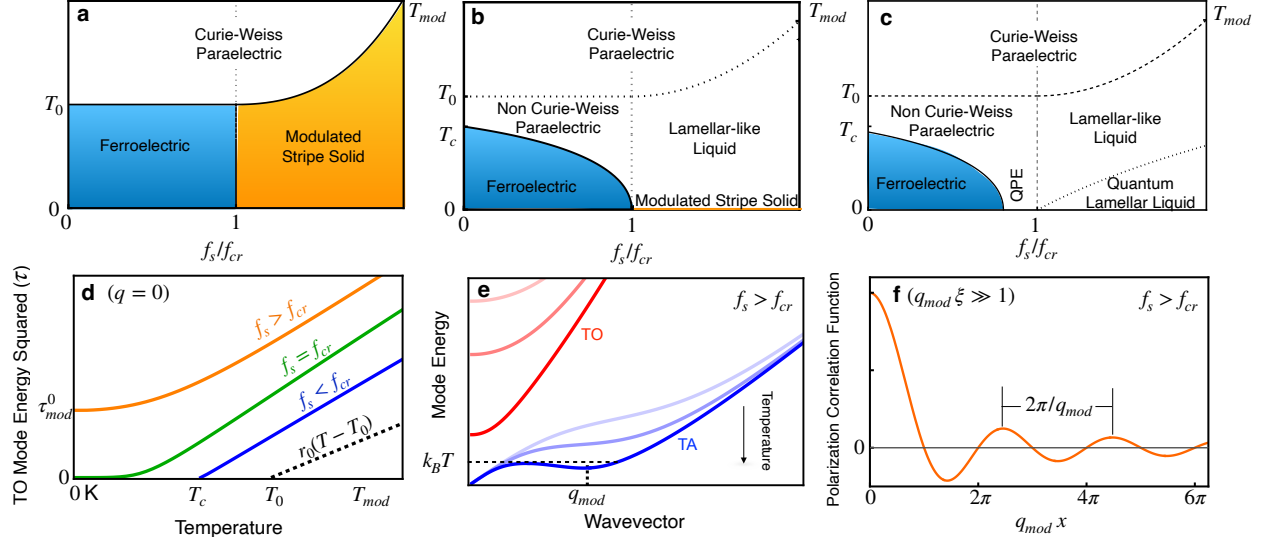


FIG. 1. Phase boundaries in the (a) harmonic approximation and in the SCPA (b) ignoring and (c) including quantum fluctuations of polarization. (d) SCPA schematics of the temperature dependence of the zone-centre hybrid TO mode and the (e) hybrid TA and TO phonon dispersions in the disordered phase. (f) Schematic correlation function of polarization in the lamellar-like liquid with correlation length ξ (see Eq. (2)). QPE=quantum paraelectric.

polarization and strain inhomogeneity. In the underlying ordered phase, the rotational symmetry of the crystal is broken as well as its translational symmetry, but only in one direction (\mathbf{q}_{mod}). This would lead to intertwined stripe order parameters where the polarization and elastic strain are periodic with a wavevector \mathbf{q}_{mod} [31]. Such stratified ordering resembles the structural organisation of the “lamellar” or “smectic” phases in liquid crystals: a nearly periodic array of parallel layers of polarizable molecules which do not possess long-range positional order within a layer [34]. In a smectic the director vector \mathbf{n} points orthogonal to the planar lamellae, as does here the wavevector \mathbf{q}_{mod} . The underlying materials science is of course quite different.

Lastly, we comment on lacunae in the model, the most important of which is the neglect of crystal anisotropy and compositional disorder. We expect anisotropy to lead to an ordered (striped) phase at low enough temperatures; disorder to a glassy frozen version of the same. Both of these effects can suppress the quantum regime. We also suggest experiments to further test our proposed picture.

We consider an isotropic polarizable, elastic medium with a polarization order parameter $P_\alpha(\mathbf{x})$ and a linear strain $\epsilon_{\alpha\beta}(\mathbf{x}) = (1/2)(\partial u_\alpha/\partial x_\beta + \partial u_\beta/\partial x_\alpha)$ as a secondary order parameter in which $u_\alpha(\mathbf{x})$ is the displacement field due to long-wavelength acoustic phonons

($\alpha, \beta = 1, 2, 3$). $P_\alpha(\mathbf{x})$ is associated with a soft transverse optic (TO) mode, the condensation of which leads to the FE transition. This leads us to consider the GL Hamiltonian that is a sum of three terms: for the polarization H_{pol} ; the elastic modes H_{elastic} ; and the static flexoelectric coupling H_{flexo} [2],

$$H = H_{\text{pol}} + H_{\text{elastic}} + H_{\text{flexo}}, \quad (1)$$

where,

$$H_{\text{pol}} = \frac{1}{2} \int d^3x d^3x' \sum_{\alpha, \beta} U_{\alpha\beta}(\mathbf{x}, \mathbf{x}') P_\alpha(\mathbf{x}) P_\beta(\mathbf{x}') + u \int d^3x \sum_{\alpha, \beta} P_\alpha^2(\mathbf{x}) P_\beta^2(\mathbf{x}),$$

$$H_{\text{elastic}} = \frac{1}{2} \int d^3x \sum_{\alpha, \beta, \gamma, \lambda} C_{\alpha\beta\gamma\lambda} \epsilon_{\alpha\beta}(\mathbf{x}) \epsilon_{\gamma\lambda}(\mathbf{x}),$$

and,

$$H_{\text{flexo}} = \frac{1}{2} \int d^3x \sum_{\alpha\beta\gamma\lambda} f_{\alpha\beta\gamma\lambda} \left[\epsilon_{\beta\gamma}(\mathbf{x}) \frac{\partial P_\alpha(\mathbf{x})}{\partial x_\lambda} - P_\alpha(\mathbf{x}) \frac{\partial \epsilon_{\beta\gamma}(\mathbf{x})}{\partial x_\lambda} \right].$$

Here, $U_{\alpha\beta}(\mathbf{x}, \mathbf{x}') = r\delta_{\alpha\beta}\delta(\mathbf{x} - \mathbf{x}') + F_{\alpha\beta}(\mathbf{x}, \mathbf{x}')$ is the bare propagator of the optic phonons, $F_{\alpha\beta}(\mathbf{x}, \mathbf{x}')$ is the dipole tensor with Fourier transform $F_{\alpha\beta}(\mathbf{q}) = cq^2\delta_{\alpha\beta} + g_0(q_\alpha q_\beta/q^2) - h_0q_\alpha q_\beta$ [35]. $C_{\alpha\beta\gamma\delta}$ is the elastic constant tensor in units of energy per unit volume, $f_{\alpha\beta\gamma\lambda}$ is the flexocoupling tensor, and $r = r_0(T - T_0)$ where T_0 is the mean field transition temperature to a homogeneous FE state at $f_{\alpha\beta\gamma\lambda} = 0$.

In the absence of flexoelectric coupling and non-linearities ($u = 0$), the phonon excitations of H are well-known: there are two doubly-fold degenerate TO and TA modes with (squared) frequencies $\omega_{\text{TO}}^2(\mathbf{q}) = r + cq^2$ and $\omega_{\text{TA}}^2(\mathbf{q}) = (\hbar^2 C_s/\rho)q^2$, respectively, and two singly-degenerate longitudinal optic and acoustic modes with (squared) frequencies $\omega_{\text{LO}}^2(\mathbf{q}) = r + g_0 + (c + h_0)q^2$ and $\omega_{\text{LA}}^2(\mathbf{q}) = (\hbar^2(C_v + (4/3)C_s)/\rho)q^2$, respectively. C_v and C_s are the bulk and shear elastic moduli, respectively, and ρ is the density of the solid.

In this paper, we focus on the effects on the hybrid transverse modes only as the level repulsion is significantly weaker in the longitudinal branches due to the characteristically large depolarizing fields of FEs which gap the longitudinal optic excitations. Moreover,

it is shown in the Supplementary Note 1 (SN1) that in isotropic media the flexoelectric interaction does not mix the transverse and longitudinal excitations.

We now discuss our results. Figure 1 (a) shows schematics of the phase boundary (PB) computed from the condensation of the bare modes (i.e., $u = 0$) in the parent phase (see SN1). For small shears of the flexocoupling tensor (i.e., $f_s < f_{cr} = \sqrt{cC_s}$), the soft zone-center TO mode condenses at a transition temperature which is independent of f_s and equal to T_0 , thus leading to a FE transition. For large flexoelectric shears (i.e., $f_s > f_{cr}$), a soft minimum develops at a non-zero wave-vector \mathbf{q}_{mod} of the TA branch, which upon condensation at a temperature $T_{mod} > T_0$, would lead to the modulated phase with coupled strain and polarization order parameters that are periodic with a wavevector \mathbf{q}_{mod} [31]. The zone-center TO mode remains gaped with energy squared $\tau_{mod}^0 \equiv r_0(T_{mod} - T_0)$. At $f_s = f_{cr}$, $\mathbf{q}_{mod} = 0$ and both the TO and TA modes condense $T_{mod} = T_0$.

We now assess the stability of the bare PB. Near above T_0 and T_{mod} and in the classical limit, the local correlation functions of polarization are approximately given as follows (see SN2),

$$\langle \mathbf{P}^2 \rangle_0 \propto \begin{cases} 1 - b(T - T_0)^{1/2}, & f_s < f_{cr}, \\ (T - T_0)^{-1/4}, & f_s = f_{cr}, \\ (T - T_{mod})^{-1/2}, & f_s > f_{cr}, \end{cases}$$

where $\langle \dots \rangle_0$ denotes thermal average at the Gaussian level and b is a constant. The PB is thus strongly modified by the inclusion of fluctuations: while the FE transition prevails at T_0 , the long-range modulated phase change is unstable, except at absolute zero where $\langle \mathbf{P}^2 \rangle_0 = 0$.

We now consider non-linearities (i.e., $u > 0$) in the SCPA (see SN3). We first discuss the impact of thermal fluctuations alone and then introduce quantum effects. Fig. 1 (b) shows the purely classical PB. For $f_s < f_{cr}$, the coupling to finite momentum elastic fluctuations suppresses the FE transition temperature and leads to a thermal regime where the squared of the soft zone-center TO phonon frequency τ (or equivalently the inverse dielectric constant) separates from the CW law behavior, as shown in Fig. 1 (d). For $f_s > f_{cr}$, the bare PB turns into a crossover. This is illustrated best by the SCPA dispersions shown in Fig. 1 (d). As mentioned above, the bare coupled acoustic mode softens to zero at a non-zero momentum

\mathbf{q}_{mod} . However, in an isotropic theory, such as ours, only the modulus of \mathbf{q}_{mod} is determined but not the direction. The phase space for fluctuations in the *direction* of \mathbf{q}_{mod} lies on the surface of a sphere of one dimension less than the physical dimension. This all but guarantees that thermal fluctuations *at any finite temperature* will disorder the direction, so there will be no long-range stripe order. This is very analogous to fluctuating laminar or nematic soft matter systems [34]. Consequently, the harmonic transition in Fig. 1(a) becomes a crossover in Fig. 1(b), and the acoustic excitations in the vicinity of \mathbf{q}_{mod} acquire a gap, as seen in Fig. 1(e). The polarization correlations of the melted phase are sinusoidal functions attenuated by an exponentially decaying envelope with a correlation length $\xi \propto (\tau - \tau_{mod}^0)^{-1/4}$ longer than the period of the modulation, i.e.,

$$\langle \mathbf{P}(\mathbf{x}) \cdot \mathbf{P}(\mathbf{0}) \rangle \sim e^{-x/(2q_{mod}\xi^2)} \sin(q_{mod}x) / (q_{mod}x), \quad (q_{mod}\xi \gg 1), \quad (2)$$

where $x = |\mathbf{x}|$ and $q_{mod} = |\mathbf{q}_{mod}|$ (see SN3). This is schematically shown in Fig. 1(f). Upon cooling, ξ would grow as τ approaches τ_{mod}^0 (Fig. 1(d)) and diverge at absolute zero, thus restoring the long-range stripe order, as shown in Fig. 1(b).

We now assess the effects of quantum polarization fluctuations. In our model, the nonlinearity of the theory is controlled by the quartic coefficient u , as shown in Fig. 2. For $f_s = 0$, the FE transition temperature drops approximately linearly in u , vanishing at a quantum critical point. For $0 < f_s < f_{cr}$, the critical nonlinearity is reduced, and there is a much more substantial parameter regime where quantum fluctuations alone destroy the transition and lead to the standard QPE phase, as it is shown in Fig. 1(c). This is consistent with the much larger phase space for orientational fluctuations when the long-range modulated order would be at finite q .

For $f_s > f_{cr}$, the zero-point fluctuations keep the energy gap at \mathbf{q}_{mod} open even at absolute zero, thus destabilising the classical $T = 0$ K transition shown in Fig. 1(b). In addition, the temperature at which the quantum fluctuations become relevant marks another crossover in the spectrum, where the correlation length will saturate. This occurs when $k_B T$ is comparable to the energy of the excitations around \mathbf{q}_{mod} , as shown in Fig. 1(e). So, for $f_s > f_{cr}$ we predict that there will be two crossovers as T is lowered, and no long-range stripe order, as shown in Fig. 1(c). We stress that when zero-point quantum fluctuations are included, the only ordered phase that we find is ferroelectricity. But outside the envelope

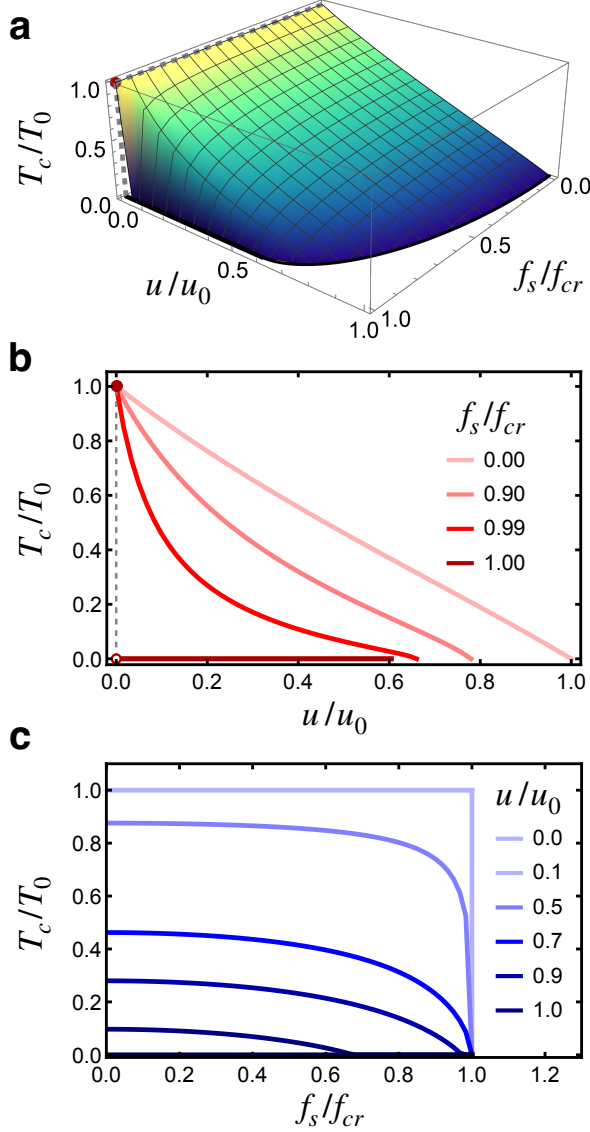


FIG. 2. (a) Dependence of the ferroelectric transition temperature T_c on the flexoelectric shear coupling constant f_s and the quartic anharmonic coefficient u of the polarization. (b)-(c) Cross-sections of (a) in the $T_c - u$ and $T_c - f_s$ plane, respectively. u_0 is the value of u at $T_c = 0$ K and $f_s = 0$.

shown in Figure 2(a) and for $f_s > f_{cr}$, we expect the lamellar-like fluctuations to have a very long-range correlation.

We now turn to comparisons to STO and KTO. Table I gives the values for the model parameters, which for the most part were taken from the literature while others were obtained from experimental data, e.g., f_s was fitted to the reported TA anomalies (0.025 rlu for STO [27], and 0.1 rlu for KTO [6]). The details can be found in SN4. For both materials, we find agreement between the calculated and measured temperature dependence of the TO

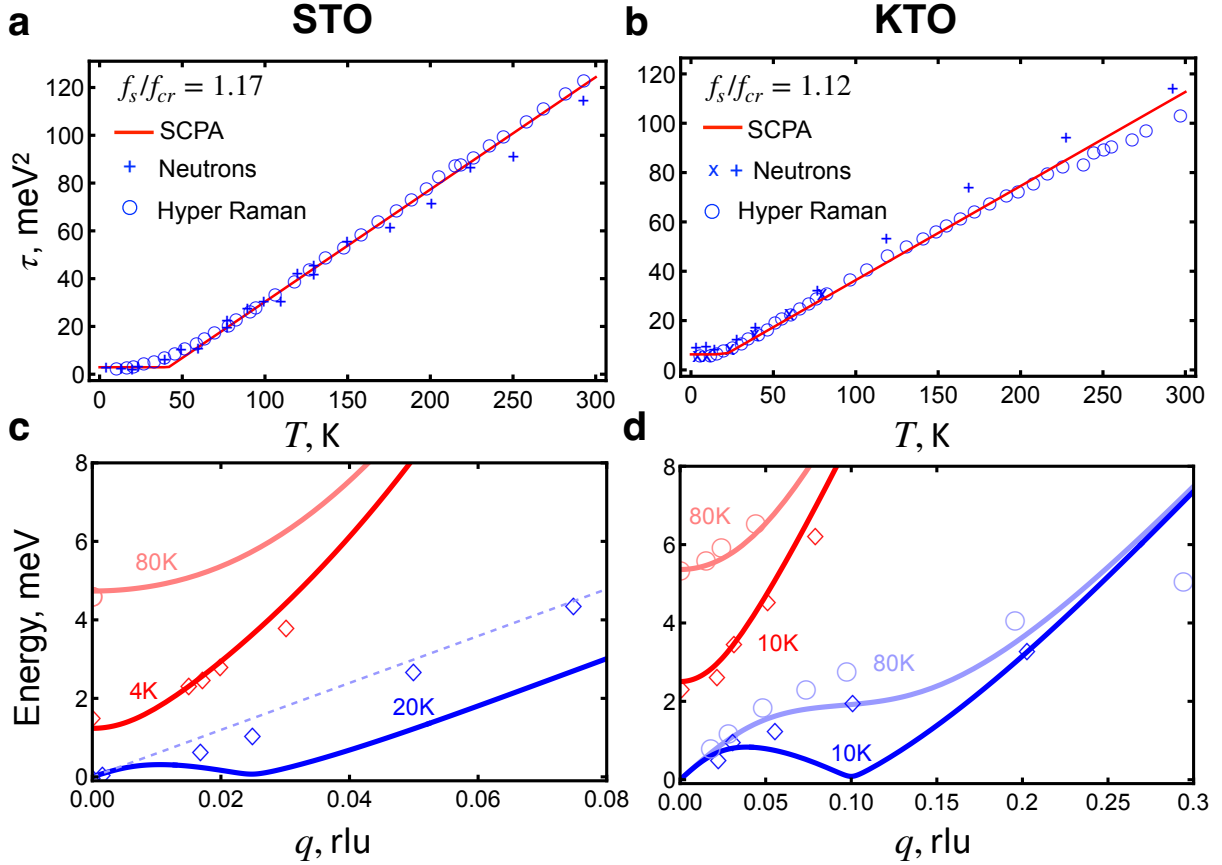


FIG. 3. (a),(b) Calculated temperature dependence of the zone center hybrid TO mode compared to neutron [36–38] and hyper-Raman [39] scattering experiments. (c),(d) Calculated dispersion of the hybrid TA and TO phonons (solid lines) compared to neutron scattering experiments (circles and diamonds) [27, 38]. Dashed line in (d) is the bare linear TA dispersion for $f_s = 0$ with a sound velocity of 4800 m/s (as shown in Ref. [27] for comparison). Model parameters are given in Table I.

frequency, as shown in Figs. 3(a) and 3(b). We note the apparent kink in the calculated frequencies is a consequence of the small values of u in our parametrization. As shown in SN3, τ is a smooth function of T at all temperatures. Figures 3(c) and 3(d) show the calculated and observed phonon dispersion curves. While our model and parametrization clearly overestimate the repulsion between the TA and TO branches, it generates a minimum at a finite q in the hybrid acoustic dispersion while preventing symmetry breaking down to the lowest temperatures, as observed in experiments [6, 27]. We stress that no such behavior occurs for $f_s \leq f_{cr}$, nor could we obtain a physically reasonable parametrization in this regime, as explained in SN4. We attribute the quantitative discrepancies to ignoring crystal anisotropy (e.g. low temperature STO is tetragonal while KTO is cubic), broadening, non-zero lifetimes, electrostriction, and coupling to other lattice modes (e.g., rotations of the

TABLE I. Model parameters.

	KTO	STO
r_0 [meV ² K ⁻¹]	0.38 ^b	0.47 ^e
T_0 [K]	4.54 ^b	35.5 ^e
u [10 ⁻⁴ meV ³ rlu ⁻³]	7.19 ^c	7.61 ^e
c [10 ³ meV ² rlu ⁻²]	4.828 ^d	13.5
a_t ^a [10 ³ meV ² rlu ⁻²]	1.553 ^d	2.739 ^f
v_t ^a [10 ³ meV ² rlu ⁻²]	3.067	6.737
h [10 ⁴ meV ⁴ rlu ⁻⁴]	6.15	406
$v_t/v_{cr} = f_s/f_{cr}$	1.12	1.17

^a $a_t = \hbar^2 C_s / \rho$ and $v_t = \hbar f_s / \sqrt{\rho}$.

^b From Ref. [40].

^c From Ref. [41].

^d From Ref. [38].

^e From Ref. [42].

^f From Ref. [43].

TiO₆ octahedra). Our fits place both materials in the liquid phase of Fig. 1 (c) ($f_s/f_{cr} = 1.17$ for STO and $f_s/f_{cr} = 1.12$ for KTO). Of course, these values should be taken as rough estimates, as our simplified model, approximate solution, and currently available experimental data prevent us from determining f_s precisely. Nonetheless, they show that both materials are near a modulated instability.

This point of course connects to a long debate about the nature of the FE phase transition as “displacive” or “order-disorder” [44, 45]. Polar nanodomains are clearly seen at room temperature in strained (and therefore low-temperature ferroelectric) films of STO though their presence has been attributed to long-range Coulomb forces rather than strain [46]. Nuclear magnetic resonance (NMR) is a technique that is sensitive to local charge disproportionation and electric field gradients, and was useful in identifying charge-density waves in transition metal dichalcogenides, even when not fully ordered [47, 48]. NMR measurements on STO [49] have been interpreted in terms of dynamic fluctuations of the Ti-ion into off-center sites coupled in a biased way to elongations of the unit cell; however the length scale of this correlation could not be determined and the measurements did not go below 25 K. Data at a lower temperature would be helpful. Ab initio calculations of STO [50] concluded that quantum lattice fluctuations are necessary to stabilise the paraelectric phase - but spatially modulated phases were not considered in that work. Modulated phases could also be in principle seen in ab initio calculations, albeit using very large supercells. In

that context we note recent calculations [51, 52] which predict that STO and cubic BaTiO₃ should be polymorphic at $T = 0$ K, with a disordered arrangement of off-site Ti distortions. A disordered ground state at absolute zero violates the third law, and perhaps is associated instead with the failure to match the supercell to the natural incommensurate period.

We now discuss our simplifying approximations. We have ignored crystal anisotropy, in which case the orientational modes will have a preferred direction. Once the temperature becomes considerably smaller than the anisotropy in the spectrum, the phase space volume of critical fluctuations will be reduced, which may lead to the stabilization of an ordered modulated phase which could precede the establishment of an ordered FE phase (this is of course the standard situation seen, for example, in quartz [53]). Similarly, disorder will break the $\mathcal{O}(3)$ symmetry and should be expected to lead to a glassy phase where orientational fluctuations are frozen. This is a familiar situation in, e.g. charge-density-wave systems, where impurities and disorder pin its order parameter and generate a strongly nonlinear response to applied electric fields [54, 55]. Our conclusion that STO should be near a modulated instability is in stark contrast with ab initio calculations [56], which suggest that $f_s/f_{cr} \simeq 0.7$ at most. We note, however, that we are using a phenomenological continuum theory where the parameters are determined from experiment (but nonetheless can make explicit predictions because the number of parameters is small). We cannot assert that the parameters can be directly calculated from harmonic microscopic theory because we have already coarse-grained to a scale of many unit cells, so that, for example, twin boundaries and defect structures have been integrated over [57]. Therefore, the difference between parameters obtained from macroscopic fits and those determined by microscopic calculations hints at some mesoscale physics to be unearthed.

Our self-consistent harmonic solution of the model implicitly assumes that in the melted phases the amplitudes of fluctuations are small. Beyond this regime, electrostrictive couplings (effectively quartic in the primary order parameter) will be important. These of course enhance the anisotropy (at least at very long length scales) but also effectively soften the sound velocity and hence enhance the flexoelectric effect. In a strong coupling theory, the model would become one of quasi-periodic FE domains separated by fluctuating, sharp domain walls. In a better theory, the modes will acquire a linewidth, as seen in experiment. This is an interesting matter for future exploration, but we expect that the qualitative features of our theory should survive.

We conclude that a strong enough flexoelectric coupling and purely thermal fluctuations of polarization can mimic quantum paraelectricity by saturating the low-temperature dielectric constant. We explain that in an isotropic system, the divergent orientational fluctuations will suppress ordering even at low temperatures so that one should expect a series of crossovers upon cooling: from a high-temperature CW law; to a classical fluctuating lamellar phase; to a quantum lamellar phase; and finally to a striped phase when crystal anisotropy becomes important. Such a sequence of crossovers is loosely consistent with experiments in STO [23, 24] and the soft finite q modes have also been observed [27, 28]. Coak *et al.* [23] ventured that a loss peak seen in their data might be ascribed to quantum fluctuations of domain walls. We also stress that the quantum regime of our theory does not require tunneling of heavy atoms through potential barriers, but is simply zero-point physics in a quasi-harmonic well. With an albeit simplified theory, our parameters are physically reasonable and we believe our model provides a fair description of the disordered state in STO and KTO.

In addition to the NMR experiments suggested above to further test our proposed scenario, we point out that measurements of the dynamical structure factor $S(\mathbf{q}, \omega)$ would detect fluctuations associated with the melting of the modulated phase. $S(\mathbf{q}, \omega)$ has of course been measured by neutrons and X-rays in STO [29, 37, 58] and KTO [6, 38], but more data is needed in order to clearly resolve any dips along their acoustic branches. Finally, we point out that our model could be adapted to investigate flexoelectricity in other systems such as recently synthesized complex oxide membranes [59], has a relation to structural Leggett modes in pyrochlore relaxors [60], and could be relevant to metallicity and superconductivity in doped STO [61].

We acknowledge helpful feedback from Benoît Fauqué, Massimiliano Stengel, Peter Abamonte, Caitlin Kengle, Michael Norman, Xing He, and Siddharth Saxena. C.H.L. acknowledges support from NSF GRFP DGE-1746045, NSF INTERN, and DOE SCGSR. G.G.G.-V. acknowledges support from the Vice-rectory for Research at the University of Costa Rica under project No. 816-C1-601.

-
- [1] P. Zubko, G. Catalan, and A. K. Tagantsev, Flexoelectric effect in solids, *Ann. Rev. Mater. Res.* **43**, 387 (2013).
- [2] P. V. Yudin and A. K. Tagantsev, Fundamentals of flexoelectricity in solids, *Nanotechnology* **24**, 432001 (2013).
- [3] A. K. Tagantsev and P. V. Yudin, eds., *Flexoelectricity in Solids: From Theory to Applications* (World Scientific, 2016).
- [4] B. Wang, Y. Gu, S. Zhang, and L.-Q. Chen, Flexoelectricity in solids: Progress, challenges, and perspectives, *Prog. Mater. Sci.* **106**, 100570 (2019).
- [5] V. G. Vaks, Phase transitions of the displacement type in ferroelectrics, *J. Exp. Th. Phys.* **27**, 486 (1968).
- [6] J. D. Axe, J. Harada, and G. Shirane, Anomalous acoustic dispersion in centrosymmetric crystals with soft optic phonons, *Phys. Rev. B* **1**, 1227 (1970).
- [7] T. A. Aslanyan and A. P. Levanyuk, Possibility of formation of an incommensurate structure due to fluctuation effects, *Sov. Phys. Solid State* **22**, 1262 (1980).
- [8] V. Heine and J. D. C. McConnell, Origin of modulated incommensurate phases in insulators, *Phys. Rev. Lett.* **46**, 1092 (1981).
- [9] P. V. Yudin, R. Ahluwalia, and A. K. Tagantsev, Upper bounds for flexoelectric coefficients in ferroelectrics, *Appl. Phys. Lett.* **104**, 082913 (2014).
- [10] A. N. Morozovska, E. A. Eliseev, C. M. Scherbakov, and Y. M. Vysochanskii, Influence of elastic strain gradient on the upper limit of flexocoupling strength, spatially modulated phases, and soft phonon dispersion in ferroics, *Phys. Rev. B* **94**, 174112 (2016).
- [11] B. A. Strukov and A. P. Levanyuk, *Ferroelectric Phenomena in Crystals: Physical Foundations* (Springer, 1998).
- [12] K. A. Müller and H. Burkard, SrTiO₃: An intrinsic quantum paraelectric below 4 K, *Phys. Rev. B* **19**, 3593 (1979).
- [13] K. Müller, W. Berlinger, and E. Tosatti, Indication for a novel phase in the quantum paraelectric regime of SrTiO₃, *Z. Physik B - Condensed Matter* **84**, 277 (1991).
- [14] R. Martoňák, *New Phenomena in the Quantum Paraelectric State of SrTiO₃*, Master's thesis, International School for Advanced Studies (1991).

- [15] E. Tosatti and R. Martoňák, Rotational melting in displacive quantum paraelectrics, [Solid State Communications](#) **92**, 167 (1994).
- [16] R. Martoňák and E. Tosatti, Path-integral monte carlo study of a model two-dimensional quantum paraelectric, [Phys. Rev. B](#) **49**, 12596 (1994).
- [17] W. Zhong and D. Vanderbilt, Effect of quantum fluctuations on structural phase transitions in SrTiO₃ and BaTiO₃, [Phys. Rev. B](#) **53**, 5047 (1996).
- [18] R. Roussev and A. J. Millis, Theory of the quantum paraelectric-ferroelectric transition, [Phys. Rev. B](#) **67**, 014105 (2003).
- [19] A. Bussmann-Holder, H. Büttner, and A. R. Bishop, Polar-soft-mode-driven structural phase transition in SrTiO₃, [Phys. Rev. Lett.](#) **99**, 167603 (2007).
- [20] L. Pálová, P. Chandra, and P. Coleman, Quantum critical paraelectrics and the casimir effect in time, [Phys. Rev. B](#) **79**, 075101 (2009).
- [21] G. J. Conduit and B. D. Simons, Theory of quantum paraelectrics and the metaelectric transition, [Phys. Rev. B](#) **81**, 024102 (2010).
- [22] P. Chandra, G. G. Lonzarich, S. E. Rowley, and J. F. Scott, Prospects and applications near ferroelectric quantum phase transitions: a key issues review, [Rep. Prog. Phys.](#) **80**, 112502 (2017).
- [23] M. J. Coak, C. R. S. Haines, C. Liu, D. M. Jarvis, P. B. Littlewood, and S. S. Saxena, Dielectric response of quantum critical ferroelectric as a function of pressure, [Sci. Rep.](#) **8**, 14936 (2018).
- [24] M. J. Coak, C. R. S. Haines, C. Liu, S. E. Rowley, G. G. Lonzarich, and S. S. Saxena, Quantum critical phenomena in a compressible displacive ferroelectric, [Proc. Natl. Acad. Sci.](#) **117**, 12707 (2020).
- [25] M. J. Coak, C. R. S. Haines, C. Liu, G. G. Guzmán-Verri, and S. S. Saxena, Pressure dependence of ferroelectric quantum critical fluctuations, [Phys. Rev. B](#) **100**, 214111 (2019).
- [26] S. E. Rowley, L. J. Spalek, R. P. Smith, M. P. M. Dean, M. Itoh, J. F. Scott, G. G. Lonzarich, and S. S. Saxena, Ferroelectric quantum criticality, [Nature Phys.](#) **10**, 367 (2014).
- [27] B. Fauqué, P. Bourges, A. Subedi, K. Behnia, B. Baptiste, B. Roessli, T. Fennell, S. Raymond, and P. Steffens, Mesoscopic fluctuating domains in strontium titanate, [Phys. Rev. B](#) **106**, L140301 (2022).
- [28] C. S. Kengle, S. I. Rubeck, M. Rak, J. Chen, F. Hoveyda, S. Bettler, A. Husain, M. Mitrano, A. Edelman, P. Littlewood, T.-C. Chiang, F. Mahmood, and P. Abbamonte, [Anharmonic](#)

- multi-phonon origin of the valence plasmon in $\text{SrTi}_{1-x}\text{Nb}_x\text{O}_3$ (2022), [arXiv:2210.15026](https://arxiv.org/abs/2210.15026).
- [29] R. Vacher, J. Pelous, B. Hennion, G. Coddens, E. Courtens, and K. A. Müller, Anomalies in the TA-Phonon Branches of SrTiO_3 in the Quantum Paraelectric Regime, [Europhys. Lett.](#) **17**, 45 (1992).
- [30] See Fig. 2 in Supplementary of Ref. [58].
- [31] R. Blinc and A. P. Levanyuk, eds., *Incommensurate phases in dielectrics*, Vol. 1 & 2 (Elsevier, 1986).
- [32] J. F. Scott, Acoustic-phonon dispersion at incommensurate phase transitions, [Ferroelectrics](#) **47**, 33 (1983).
- [33] V. Heine and J. D. C. McConnell, The origin of incommensurate structures in insulators, [J. Phys. C: Solid State Physics](#) **17**, 1199 (1984).
- [34] P. M. Chaikin and T. C. Lubensky, *Principles of Condensed Matter Physics* (Cambridge University Press, 1995).
- [35] A. Aharony and M. E. Fisher, Critical behavior of magnets with dipolar interactions. i. renormalization group near four dimensions, [Phys. Rev. B](#) **8**, 3323 (1973).
- [36] G. Shirane, R. Nathans, and V. J. Minkiewicz, Temperature dependence of the soft ferroelectric mode in KTaO_3 , [Phys. Rev.](#) **157**, 396 (1967).
- [37] Y. Yamada and G. Shirane, Neutron scattering and nature of the soft optical phonon in SrTiO_3 , [J. Phys. Soc. Jpn.](#) **26**, 396 (1969).
- [38] E. Farhi, A. K. Tagantsev, R. Currat, B. Hehlen, E. Courtens, and L. A. Boatner, Low energy phonon spectrum and its parameterization in pure KTaO_3 below 80 K, [Eur. Phys. J. B.](#) **15**, 615 (2000).
- [39] H. Vogt, Refined treatment of the model of linearly coupled anharmonic oscillators and its application to the temperature dependence of the zone-center soft-mode frequencies of KTaO_3 and SrTiO_3 , [Phys. Rev. B](#) **51**, 8046 (1995).
- [40] H. Fujishita, S. Kitazawa, M. Saito, R. Ishisaka, H. Okamoto, and T. Yamaguchi, Quantum paraelectric states in SrTiO_3 and KTaO_3 : Barrett model, Vendik model, and quantum criticality, [J. Phys. Soc. Jpn.](#) **85**, 074703 (2016).
- [41] V. Skoromets, C. Kadlec, H. Němec, D. Fattakhova-Rohlfing, and P. Kužel, Tunable dielectric properties of KTaO_3 single crystals in the terahertz range, [J. Phys. D: Appl. Phys.](#) **49**, 065306 (2016).

- [42] K. M. Rabe, C. H. Ahn, and J.-M. Triscone, eds., *Physics of Ferroelectrics A Modern Perspective* (Springer-Verlag, 2007).
- [43] M. A. Carpenter, Elastic anomalies accompanying phase transitions in (Ca,Sr)TiO₃ perovskites: Part I. Landau theory and a calibration for SrTiO₃, *Am. Mineral* **92**, 309 (2007).
- [44] F. Jona and G. Shirane, *Ferroelectric Crystals* (Dover, 1993).
- [45] R. Comès, M. Lambert, and A. Guinier, Désordre linéaire dans les cristaux (cas du silicium, du quartz, et des pérovskites ferroélectriques), *Acta Crys.* **A26**, 244 (1970).
- [46] S. Salmani-Rezaie, K. Ahadi, W. M. Strickland, and S. Stemmer, Order-disorder ferroelectric transition of strained SrTiO₃, *Phys. Rev. Lett.* **125**, 087601 (2020).
- [47] J. A. R. Stiles and D. L. Williams, NMR measurements of phenomena related to charge density waves in NbSe₂, *J. Phys. C: Solid State Phys.* **9**, 3941 (1976).
- [48] L. Pfeiffer, R. E. Walstedt, R. F. Bell, and T. Kovacs, Temperature dependence of the orthorhombic charge-density-wave parameters in 2H-TaSe₂ by ⁷⁷Se nuclear magnetic resonance, *Phys. Rev. Lett.* **49**, 1162 (1982).
- [49] B. Zalar, A. Lebar, J. Seliger, R. Blinc, V. V. Laguta, and M. Itoh, NMR study of disorder in BaTiO₃ and SrTiO₃, *Phys. Rev. B* **71**, 064107 (2005).
- [50] D. Shin, S. Latini, C. Schäfer, S. A. Sato, U. De Giovannini, H. Hübener, and A. Rubio, Quantum paraelectric phase of SrTiO₃ from first principles, *Phys. Rev. B* **104**, L060103 (2021).
- [51] X.-G. Zhao, Z. Wang, O. I. Mal'yi, and A. Zunger, Effect of static local distortions vs. dynamic motions on the stability and band gaps of cubic oxide and halide perovskites, *Materials Today* **49**, 107 (2021).
- [52] X.-G. Zhao, O. I. Mal'yi, S. J. L. Billinge, and A. Zunger, Intrinsic local symmetry breaking in nominally cubic paraelectric BaTiO₃, *Phys. Rev. B* **105**, 224108 (2022).
- [53] T. A. Aslanyan and A. P. Levanyuk, On the possibility of the incommensurate phase near $\alpha \leftrightarrow \beta$ transition point in quartz, *Solid State Commun.* **31**, 547 (1979).
- [54] H. Fukuyama and P. A. Lee, Dynamics of the charge-density wave. I. Impurity pinning in a single chain, *Phys. Rev. B* **17**, 535 (1978).
- [55] P. A. Lee and T. M. Rice, Electric field depinning of charge density waves, *Phys. Rev. B* **19**, 3970 (1979).
- [56] M. Stengel, Unified ab initio formulation of flexoelectricity and strain-gradient elasticity, *Phys. Rev. B* **93**, 245107 (2016).

- [57] D. Pesquera, M. A. Carpenter, and E. K. H. Salje, Glasslike dynamics of polar domain walls in cryogenic SrTiO₃, [Phys. Rev. Lett. **121**, 235701 \(2018\)](#).
- [58] X. He, D. Bansal, B. Winn, S. Chi, L. Boatner, and O. Delaire, Anharmonic eigenvectors and acoustic phonon disappearance in quantum paraelectric SrTiO₃, [Phys. Rev. Lett. **124**, 145901 \(2020\)](#).
- [59] V. Harbola, S. Crossley, S. S. Hong, D. Lu, Y. A. Birkhölzer, Y. Hikita, and H. Y. Hwang, Strain gradient elasticity in SrTiO₃ membranes: bending versus stretching, [Nano Lett. **21**, 2470 \(2021\)](#).
- [60] Q. N. Meier, D. Hickox-Young, G. Laurita, N. A. Spaldin, J. M. Rondinelli, and M. R. Norman, Leggett modes accompanying crystallographic phase transitions, [Phys. Rev. X **12**, 011024 \(2022\)](#).
- [61] C. W. Rischau, X. Lin, C. P. Grams, F. Finck, S. Harms, J. Engelmayer, T. Lorenz, T. Gallais, B. Fauqué, J. Hemberger, and K. Behnia, A ferroelectric quantum phase transition inside the superconducting dome of Sr_{1-x}Ca_xTiO_{3-δ}, [Nat. Phys. **13**, 643 \(2017\)](#).

Supplementary Information

G. G. Guzmán-Verri^{1,2,3}, C. H. Liang^{4,5}, P. B. Littlewood⁴

¹*Centro de Investigación en Ciencia e Ingeniería de Materiales (CICIMA),*

Universidad de Costa Rica, San José, Costa Rica 11501,

²*Escuela de Física, Universidad de Costa Rica, San José, Costa Rica 11501,*

³*Department of Materials Science and Metallurgy, University of Cambridge, Cambridge,
UK CB3 0DS,*

⁴*James Franck Institute, University of Chicago, 929 E 57 St, Chicago, Illinois, USA 60637,*

⁵*Pritzker School of Molecular Engineering, University of Chicago, 5640 S Ellis Ave,
Chicago, Illinois, USA 60637.*

Contents

Note 1. Bare hybrid modes.

Note 2. Phase stability.

Note 3. Self-consistent phonon approximation.

Note 4. Fits to experiments in STO and KTO.

References.

SUPPLEMENTARY NOTE 1. BARE HYBRID MODES

In the absence of non-linearities ($u = 0$), we rewrite the GL Hamiltonian of Eq. (1) in momentum space and in terms of the displacement field,

$$H = \int \frac{d^3q}{(2\pi)^3} \sum_{\alpha\beta} U_{\alpha\beta}(\mathbf{q}) P_\alpha(\mathbf{q}) P_\beta^*(\mathbf{q}) + \sum_{\alpha\beta} M_{\alpha\beta}(\mathbf{q}) u_\alpha(\mathbf{q}) u_\beta^*(\mathbf{q}) + \sum_{\alpha\beta} V_{\alpha\beta}(\mathbf{q}) [u_\alpha(\mathbf{q}) P_\beta^*(\mathbf{q}) + u_\alpha^*(\mathbf{q}) P_\beta(\mathbf{q})], \quad (\text{S1})$$

where $M_{\alpha\beta}(\mathbf{q}) = \sum_{\gamma\lambda} C_{\gamma\alpha\lambda\beta} q_\gamma q_\lambda$, is the bare dynamical matrix of the acoustic phonons, and $V_{\alpha\beta}(\mathbf{q}) = \sum_{\gamma\lambda} f_{\alpha\beta\gamma\lambda} q_\gamma q_\lambda$ is the flexoelectric interaction. $\int d^3q$ indicates to integrate over half reciprocal space only.

For isotropic media [S1, S2],

$$U_{\alpha\beta}(\mathbf{q}) = [r + cq^2] \delta_{\alpha\beta} + g_0 (q_\alpha q_\beta / q^2) - h_0 q_\alpha q_\beta,$$

$$C_{\alpha\beta\gamma\lambda} = (C_v - 2C_s/3) \delta_{\alpha\beta} \delta_{\gamma\lambda} + C_s (\delta_{\alpha\gamma} \delta_{\beta\lambda} + \delta_{\alpha\lambda} \delta_{\beta\gamma}),$$

and [S3],

$$f_{\alpha\beta\gamma\lambda} = (f_v - 2f_s/3) \delta_{\alpha\lambda} \delta_{\beta\gamma} + f_s (\delta_{\alpha\gamma} \delta_{\beta\lambda} + \delta_{\alpha\beta} \delta_{\gamma\lambda}),$$

where $C_v = (C_{11} + 2C_{12})/3$ and $C_s = (C_{11} - C_{12})/2$ are the bulk and shear moduli and $f_v = (f_{11} + 2f_{12})/3$ and $f_s = (f_{11} - f_{12})/2$ are bulk and shear components of the flexocoupling tensor.

Thus,

$$M_{\alpha\beta}(\mathbf{q}) = (C_v + C_s/3) q_\alpha q_\beta + C_s q^2 \delta_{\alpha\beta},$$

and,

$$V_{\alpha\beta}(\mathbf{q}) = (f_v + f_s/3) q_\alpha q_\beta + f_s q^2 \delta_{\alpha\beta},$$

In the normal coordinates of the bare modes without flexoelectricity, the inverse propagator $\mathbf{G}_0^{-1}(\mathbf{q})$ of Eq. (S1) is block-diagonal,

$$\mathbf{G}_0^{-1}(\mathbf{q}) = \begin{pmatrix} \omega_{\text{TO}}^2(\mathbf{q}) & V_t(\mathbf{q}) & 0 & 0 & 0 & 0 \\ V_t(\mathbf{q}) & \omega_{\text{TA}}^2(\mathbf{q}) & 0 & 0 & 0 & 0 \\ 0 & 0 & \omega_{\text{TO}}^2(\mathbf{q}) & V_t(\mathbf{q}) & 0 & 0 \\ 0 & 0 & V_t(\mathbf{q}) & \omega_{\text{TA}}^2(\mathbf{q}) & 0 & 0 \\ 0 & 0 & 0 & 0 & \omega_{\text{LO}}^2(\mathbf{q}) & V_l(\mathbf{q}) \\ 0 & 0 & 0 & 0 & V_l(\mathbf{q}) & \omega_{\text{LA}}^2(\mathbf{q}) \end{pmatrix}, \quad (\text{S2})$$

where,

$$\begin{aligned} \omega_{\text{TO}}^2(\mathbf{q}) &= r + cq^2 + hq^4, & \omega_{\text{LO}}^2(\mathbf{q}) &= r + g_0 + (c + h_0)q^2, \\ \omega_{\text{TA}}^2(\mathbf{q}) &= a_tq^2, & \omega_{\text{LA}}^2(\mathbf{q}) &= a_lq^2, \\ V_t(\mathbf{q}) &= v_tq^2, & V_l(\mathbf{q}) &= v_lq^2, \end{aligned}$$

with $a_t \equiv \hbar^2 C_s / \rho$, $a_l \equiv \hbar^2 (C_v + (4/3)C_s) / \rho$, $v_t \equiv \hbar f_s / \sqrt{\rho}$, and $v_l \equiv \hbar (f_v + (4/3)f_s) / \sqrt{\rho}$, where ρ is the density in units of mass per unit volume. In writing Eq. (S2), we have chosen the following ordering for the entries of $\mathbf{G}_0^{-1}(\mathbf{q})$: $\{P_{\text{T1}}(\mathbf{q}), u_{\text{T1}}(\mathbf{q}), P_{\text{T2}}(\mathbf{q}), u_{\text{T2}}(\mathbf{q}), P_{\text{L}}(\mathbf{q}), u_{\text{L}}(\mathbf{q})\}$, where T and L refer to transverse and longitudinal components relative to \mathbf{q} , respectively. Note that $V_{\alpha\beta}(\mathbf{q})$ does not mix the transverse and longitudinal modes and that the transverse blocks are identical. These are consequences of assuming an isotropic medium and do not generally occur in crystals. Note we have added a $\mathcal{O}(q^4)$ term in $\omega_{\text{TO}}^2(\mathbf{q})$ by hand. This is done to produce a well-conditioned hybrid TA branch for $f_s > f_{cr}$ that would allow us to capture the modulated wavevector in the hybrid modes (otherwise it would be negatively unbounded, which is unphysical). We note such terms can result from higher-order gradients in the effective Hamiltonian (e.g., $|\nabla \mathbf{P}(\mathbf{x})|^4$). We do not explicitly write them down in Eq. (1) for simplicity, as it is sometimes done in the continuum theory of incommensurate transitions [S4]. We also note that a similar term could be added to $\omega_{\text{TA}}^2(\mathbf{q})$, however, we do not do so as it that would only add an extra fitting parameter with no qualitative difference in the resulting hybrid modes.

Since $G_0^{-1}(\mathbf{q})$ is a dynamical matrix, the bare frequencies are given by its eigenvalues,

$$\Omega_{\text{TO}}^0(\mathbf{q}) = \frac{1}{\sqrt{2}} \left(\omega_{\text{TA}}^2(\mathbf{q}) + \omega_{\text{TO}}^2(\mathbf{q}) + \sqrt{4V_t^2(\mathbf{q}) + [\omega_{\text{TO}}^2(\mathbf{q}) - \omega_{\text{TA}}^2(\mathbf{q})]^2} \right)^{1/2}, \quad (\text{S3a})$$

$$\Omega_{\text{TA}}^0(\mathbf{q}) = \frac{1}{\sqrt{2}} \left(\omega_{\text{TA}}^2(\mathbf{q}) + \omega_{\text{TO}}^2(\mathbf{q}) - \sqrt{4V_t^2(\mathbf{q}) + [\omega_{\text{TO}}^2(\mathbf{q}) - \omega_{\text{TA}}^2(\mathbf{q})]^2} \right)^{1/2}, \quad (\text{S3b})$$

$$\Omega_{\text{LO}}^0(\mathbf{q}) = \frac{1}{\sqrt{2}} \left(\omega_{\text{LA}}^2(\mathbf{q}) + \omega_{\text{LO}}^2(\mathbf{q}) + \sqrt{4V_l^2(\mathbf{q}) + [\omega_{\text{LO}}^2(\mathbf{q}) - \omega_{\text{LA}}^2(\mathbf{q})]^2} \right)^{1/2}, \quad (\text{S3c})$$

$$\Omega_{\text{LA}}^0(\mathbf{q}) = \frac{1}{\sqrt{2}} \left(\omega_{\text{LA}}^2(\mathbf{q}) + \omega_{\text{LO}}^2(\mathbf{q}) - \sqrt{4V_l^2(\mathbf{q}) + [\omega_{\text{LO}}^2(\mathbf{q}) - \omega_{\text{LA}}^2(\mathbf{q})]^2} \right)^{1/2}, \quad (\text{S3d})$$

where the transverse and longitudinal branches are two- and one-fold degenerate, respectively. The TA, TO, LA, and LO labels refer to optic- and acoustic-like mode behavior in the long-wavelength limit.

We now discuss the behavior of the hybrid modes. For $0 < v_t < v_{cr} \equiv \sqrt{c a_t}$, the TA and TO phonons repel at finite wavevectors and soften as $T \rightarrow T_0$. At T_0 , $\Omega_{\text{TO}}^0(\mathbf{q} = 0)$ condenses, which leads to a FE transition. For $v_t \geq v_{cr}$, the level repulsion generates a minimum at a finite wavevector q_{mod} in the acoustic branch as temperature decreases. At a temperature $T_{mod} = T_0 + (v_t^2 - v_{cr}^2)/(4hr_0 a_t^2)$, $q_{mod} = \sqrt{(v_t^2 - v_{cr}^2)/(2ha_t)}$ and $\Omega_{\text{TA}}^0(\mathbf{q}_{mod})$ condenses, while the zone-center TO phonon remains gaped with energy $\tau_{mod}^0 \equiv \Omega_{\text{TO}}^0(\mathbf{q} = 0) = \sqrt{r_0(T_{mod} - T_0)} = (v_{cr}^2 - v_t^2)/(2a_t\sqrt{h})$. We note that $v_t = v_{cr}$ is a triple point between the paraelectric, FE and modulated phases. N.B.: since $f_s/f_{cr} = v_t/v_{cr}$, where $f_{cr} = \sqrt{c C_s}$, the above results can be rewritten as follows: $T_{mod} = T_0 + (f_s^2 - f_{cr}^2)^2/(4hr_0 C_s^2)$, $q_{mod} = \sqrt{(f_s^2 - f_{cr}^2)/(2hC_s)}$, $\Omega_{\text{TO}}^0(\mathbf{q} = 0) = (f_{cr}^2 - f_s^2)/(2C_s\sqrt{h})$. These resulting phase diagram is shown in Fig. 1 (a).

For the longitudinal modes, the relevant parameter is v_l : for $0 \leq v_l < v_{l,cr} \equiv \sqrt{(c + h_0) a_l}$, the zone center LO phonon does not condense due to the depolarizing field g_0 . For $v_l \geq v_{l,cr}$, $\Omega_{\text{LA}}^0(\mathbf{q}_{l,mod})$ condenses at a temperature $T_{l,mod} = T_0 - (g_0/r_0) + (v_l^2 - v_{l,cr}^2)^2/(4ha_l^2 r_0)$, where $q_{l,mod} = \sqrt{(v_l^2 - v_{l,cr}^2)/(2a_l h)}$. The zone-center LO phonon remains gaped with (squared) energy $\Omega_{\text{LO}}^0(\mathbf{q} = 0) = (v_{l,cr}^2 - v_l^2)/(2a_l\sqrt{h})$. We note that T_{mod} and $T_{l,mod}$ depend for the most part on independent model parameters, therefore one cannot conclude in general which modulated transition precedes the other. Nonetheless, g_0 is typically very large in perovskite FEs, thus we expect $T_{mod} > T_{l,mod}$, which will be assumed hereafter.

SUPPLEMENTARY NOTE 2. PHASE STABILITY

We now discuss the stability of the PB. We will show that in the presence of purely thermal fluctuations the FE PB is stable, while the modulated solid and triple point in the phase diagram are unstable.

At the Gaussian level and in the classical limit, the local correlation functions $\langle |\mathbf{P}^2| \rangle$ of the disordered phase of our isotropic model are given in terms of its transverse ($\langle P_{\perp}^2(\mathbf{q}) \rangle_0 \equiv \langle P_{T1}^2(\mathbf{q}) \rangle_0 = \langle P_{T2}^2(\mathbf{q}) \rangle_0$) and longitudinal fluctuations ($\langle P_{\parallel}^2(\mathbf{q}) \rangle_0 \equiv \langle P_L^2(\mathbf{q}) \rangle_0$) as follows,

$$\langle |\mathbf{P}^2| \rangle_0 = \int \frac{d^3q}{(2\pi)^3} \left[2 \langle P_{\perp}^2(\mathbf{q}) \rangle_0 + \langle P_{\parallel}^2(\mathbf{q}) \rangle_0 \right], \quad (\text{S4})$$

where,

$$\langle P_{\perp}^2(\mathbf{q}) \rangle_0 = \frac{k_B T}{r_0(T - T_0) + (1 - v_t^2/v_{cr}^2)cq^2 + hq^4},$$

and,

$$\langle P_{\parallel}^2(\mathbf{q}) \rangle_0 = \frac{k_B T}{r_0(T - T_0) + g_0 + (1 - v_t^2/v_{l,cr}^2)(c + h_0)q^2 + hq^4}.$$

At the onset of the FE transition ($T \rightarrow T_0$ for $0 \leq v_t < v_{cr}$), $\langle P_{\perp}^2(\mathbf{q}) \rangle_0 \rightarrow \infty$ as $q \rightarrow 0$, while $\langle P_{\parallel}^2(\mathbf{q}) \rangle_0$ remains finite due to the depolarizing field term g_0 and therefore we will ignore it. By integrating $\langle P_{\perp}^2(\mathbf{q}) \rangle_0$ over all of \mathbf{q} -space, we obtain the following result for $T \rightarrow T_0$,

$$(k_B T)^{-1} \int d^3q \langle P_{\perp}^2(\mathbf{q}) \rangle_0 \propto \frac{\pi}{2\sqrt{(1 - v_t^2/v_{cr}^2)}hc} \left[1 - \sqrt{\frac{h}{c} \frac{(T - T_0)}{(1 - v_t^2/v_{cr}^2)}} \right].$$

The thermal fluctuations are finite at T_0 , thus the long-range FE order is stable in the purely classical limit.

We now look at the fluctuations near above the modulated transition. For $T \rightarrow T_{mod}$ and $v_t \geq v_{cr}$, $\langle P_{\perp}^2(\mathbf{q}) \rangle_0 \rightarrow \infty$ as $q \rightarrow q_{mod}$, whereas $\langle P_{\parallel}^2(\mathbf{q}) \rangle_0$ remains finite since $T_{mod} > T_{l,mod}$ by assumption and thus we ignore it. By integrating the transverse fluctuations over

momentum, we obtain the following result for $T \rightarrow T_{mod}$,

$$(k_B T)^{-1} \int d^3 q \langle P_{\perp}^2(\mathbf{q}) \rangle_0 \propto \left(\frac{T_{mod} - T_0}{T - T_{mod}} \right)^{1/2}. \quad (\text{S5})$$

Equation (S5) diverges as $T \rightarrow T_{mod}$, thus the modulated solid is unstable.

At the triple point ($v_t = v_{cr}$), $T_{mod} = T_0$ and $q_{mod} = 0$, thus,

$$(k_B T)^{-1} \int d^3 q \langle P_{\perp}^2(\mathbf{q}) \rangle_0 \propto \left(\frac{1}{T - T_0} \right)^{1/4}. \quad (\text{S6})$$

Equation (S6) diverges as $T \rightarrow T_0$, therefore the coexistence is unstable.

SUPPLEMENTARY NOTE 3. SELF-CONSISTENT PHONON APPROXIMATION

We follow a standard procedure [S5] to solve the statistical mechanical problem posed by our model Hamiltonian in disordered phase. At the Gaussian level, the quartic anharmonicities in Eq. (1) are approximated by,

$$\int d^3x \sum_{\alpha,\beta} u P_\alpha^2(\mathbf{x}) P_\beta^2(\mathbf{x}) \simeq \int d^3x \sum_{\alpha,\beta} [2u \langle |\mathbf{P}(\mathbf{x})|^2 \rangle \delta_{\alpha\beta} + 4u \langle P_\alpha(\mathbf{x}) P_\beta(\mathbf{x}) \rangle] P_\alpha(\mathbf{x}) P_\beta(\mathbf{x}),$$

where $\langle P_\alpha(\mathbf{x}) P_\beta(\mathbf{x}) \rangle$ are correlation functions of polarization and $\langle |\mathbf{P}(\mathbf{x})|^2 \rangle = \sum_{\gamma=1}^3 \langle P_\gamma^2(\mathbf{x}) \rangle$. We thus have an effective Hamiltonian identical to Eq. (1), but with $U_{\alpha\beta}(\mathbf{x}, \mathbf{x}')$ now given as follows,

$$U_{\alpha\beta}(\mathbf{x}, \mathbf{x}') = [(r + 4u \langle |\mathbf{P}(\mathbf{x})|^2 \rangle) \delta_{\alpha\beta} + 8u \langle P_\alpha(\mathbf{x}) P_\beta(\mathbf{x}) \rangle] \delta(\mathbf{x} - \mathbf{x}') + F_{\alpha\beta}(\mathbf{x}, \mathbf{x}').$$

By symmetry, $\langle P_1(\mathbf{x}) P_2(\mathbf{x}) \rangle = \langle P_1(\mathbf{x}) P_3(\mathbf{x}) \rangle = \langle P_2(\mathbf{x}) P_3(\mathbf{x}) \rangle = 0$ and $\langle P_1^2(\mathbf{x}) \rangle = \langle P_2^2(\mathbf{x}) \rangle = \langle P_3^2(\mathbf{x}) \rangle = (1/3) \langle |\mathbf{P}|^2 \rangle$, thus,

$$U_{\alpha\beta}(\mathbf{x}, \mathbf{x}') = [r + (20u/3) \langle |\mathbf{P}|^2 \rangle] \delta_{\alpha\beta} \delta(\mathbf{x} - \mathbf{x}') + F_{\alpha\beta}(\mathbf{x}, \mathbf{x}'). \quad (\text{S7})$$

The dressed propagator $\mathbf{G}^{-1}(\mathbf{q})$ and frequencies $\Omega_\lambda(\mathbf{q})$, ($\lambda = \text{TO, TA, LO, LA}$) are therefore identical to their corresponding bare forms given in Eqs. (S2) and (S3) with r replaced by,

$$\tau \equiv \Omega_{\text{TO}}^2(\mathbf{q} = 0) = r + (20u/3) \langle |\mathbf{P}|^2 \rangle, \quad (\text{S8})$$

where $\Omega_{\text{TO}}(0)$ is the zone-center TO mode frequency. The correlation functions are calculated from the fluctuation-dissipation theorem [S6],

$$\langle P_\alpha(\mathbf{x}) P_\beta(\mathbf{x}') \rangle = \int \frac{d^3q}{(2\pi)^3} e^{i\mathbf{q} \cdot (\mathbf{x} - \mathbf{x}')} \sum_{\lambda\lambda'} b_{\alpha\lambda}(\mathbf{q}) \psi_{\lambda\lambda'}(\mathbf{q}) b_{\lambda'\beta}^\dagger(\mathbf{q}), \quad (\text{S9})$$

where,

$$\psi_{\lambda\lambda'}(\mathbf{q}) = \frac{1}{2\Omega_\lambda(\mathbf{q})} \coth\left(\frac{\Omega_\lambda(\mathbf{q})}{2k_B T}\right) \delta_{\lambda\lambda'},$$

and $b_{\alpha\lambda}(\mathbf{q})$ is a unitary transformation that diagonalizes $\mathbf{G}^{-1}(\mathbf{q})$. Eq. (S9) provides the self-consistency equation for $\Omega_\lambda(\mathbf{q})$.

Dependence of τ on u for $f_s > f_{cr}$

Figs. S1 (a) and (b) above show the temperature dependence of $\tau \equiv \Omega_{\text{TO}}^2(0)$ and its first derivative $d\tau/dT$ for several values of u . We first point out the dramatic change in the behavior of τ between $u = 0$ and $u > 0$ is expected as infinitesimally small fluctuations prevent long-range modulated order. We then note that for finite u , $d\tau/dT$ seems to become multi-valued at T_{mod} as $u \rightarrow 0$ (but remains finite). However, a closer inspection reveals that it is well-defined.

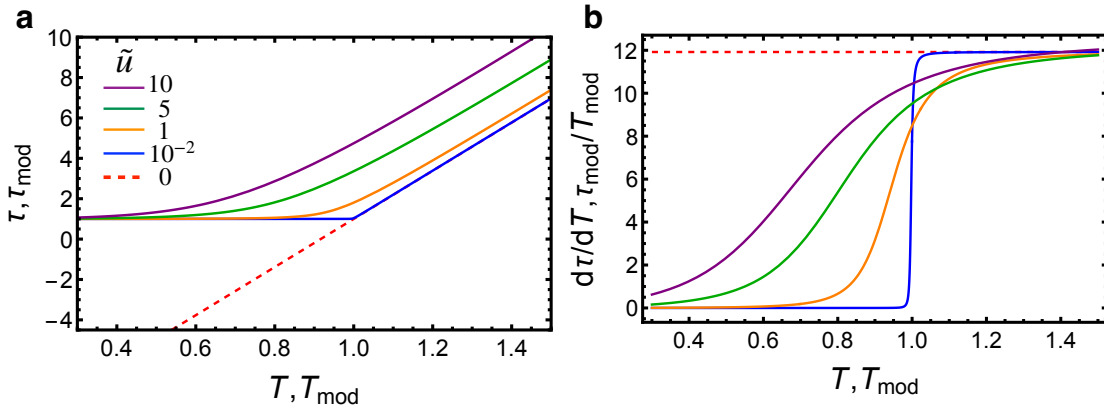


FIG. S1. (a) Temperature dependence of the zone-center TO mode τ and (b) its first derivative for several values of the dimensionless quartic coefficient $\tilde{u} \equiv (20/3\pi)(uq_{mod}^3/\sqrt{\tau_{mod}})$. All other parameters are taken from Table I of the main text for STO.

For large flexocouplings ($f_s > f_{cr}$), we rewrite Eq. (S8) as follows,

$$\tau - \tau_{mod}^0 = r_0(T - T_{mod}) + (20u/3) \langle |\mathbf{P}(0)|^2 \rangle, \quad (\text{S10})$$

where $\langle |\mathbf{P}(0)|^2 \rangle$ are the local correlation functions of polarization, and $\tau_{mod}^0 \equiv r_0(T_{mod} - T_0)$ is the harmonic ($u = 0$) zone-center TO frequency at T_{mod} .

In the classical limit and $\tau - \tau_{mod}^0 \rightarrow 0$,

$$\langle |\mathbf{P}(0)|^2 \rangle = \int \frac{d^3q}{(2\pi)^3} \frac{k_B T}{(\tau - \tau_{mod}^0) + h(q^2 - q_{mod}^2)^2} \propto \frac{k_B T}{(\tau - \tau_{mod}^0)^{1/2}}.$$

We now substitute this into Eq. (S10),

$$\tau - \tau_{mod}^0 \simeq r_0 (T - T_{mod}) + \frac{u'T}{(\tau - \tau_{mod}^0)^{1/2}},$$

with $u' \propto u$. By taking the derivative with respect to T on both sides of this equation and solve for $d\tau/dT$, we obtain the following result,

$$\frac{d\tau}{dT} = \frac{r_0 + u' / (\tau - \tau_{mod}^0)^{1/2}}{1 + u'T/2 (\tau - \tau_{mod}^0)^{3/2}}.$$

For the harmonic theory (i.e. $u' = u = 0$), we get $d\tau/dT = r_0$ at all temperatures, as expected. For $u' > 0$ and $T = T_{mod}$, $\tau - \tau_{mod}^0 \simeq (u'T_{mod})^{2/3}$ and,

$$\left. \frac{d\tau}{dT} \right|_{T=T_{mod}} = \frac{2}{3} \left(r_0 + \frac{u'^{2/3}}{T_{mod}^{1/3}} \right).$$

We thus find $d\tau/dT$ is single-valued at T_{mod} for $u' > 0$ and thus there is no kink.

Correlation function of polarization in the lamellar-like liquid phase

The purpose of this subsection is to derive the correlation function of polarization given in Eq. (2) of the main text. We consider the correlation function of polarization given as follows,

$$\langle \mathbf{P}(\mathbf{x}) \cdot \mathbf{P}(\mathbf{0}) \rangle = \sum_{\alpha} \langle P_{\alpha}(\mathbf{x}) P_{\alpha}(\mathbf{0}) \rangle = \int \frac{d^3q}{(2\pi)^3} e^{i\mathbf{q}\cdot\mathbf{x}} [2 \langle P_{\perp}^2(\mathbf{q}) \rangle + \langle P_{\parallel}^2(\mathbf{q}) \rangle], \quad (\text{S11})$$

where $\langle P_{\perp}^2(\mathbf{q}) \rangle$ and $\langle P_{\parallel}^2(\mathbf{q}) \rangle$ are transverse and longitudinal polarization correlations. In the classical limit,

$$\langle P_{\perp}^2(\mathbf{q}) \rangle = \frac{k_B T}{\tau + (1 - f_s^2/f_{cr}^2) c q^2 + h q^4}, \quad (\text{S12})$$

and,

$$\langle P_{\parallel}^2(\mathbf{q}) \rangle = \frac{k_B T}{\tau + g_0 + (1 - f_l^2/f_{l,cr}^2)(c + h_0) q^2 + h q^4}.$$

where τ is given by Eq. (S8) and q_{mod} and τ_{mod}^0 are given in SN1. Since the longitudinal fluctuations are much weaker than the transverse ones due to the large depolarizing term g_0 , we will ignore them.

For $f_s > f_{cr}$, we rewrite Eq. (S12) as follows,

$$\langle P_{\perp}^2(\mathbf{q}) \rangle = \frac{q_{mod}^4}{\tau_{mod}^0} \frac{k_B T}{\xi^{-4} + (q^2 - q_{mod}^2)^2},$$

where ξ is the correlation length,

$$q_{mod} \xi \equiv \left(\frac{\tau_{mod}^0}{\tau - \tau_{mod}^0} \right)^{1/4}.$$

Since the fluctuations are isotropic, the angular integrals in Eq. (S11) can be readily calculated,

$$\langle \mathbf{P}(\mathbf{x}) \cdot \mathbf{P}(\mathbf{0}) \rangle = \frac{k_B T}{\pi^2} \frac{q_{mod}^4}{\tau_{mod}^0} \int_0^{\infty} dq \frac{q^2}{\xi^{-4} + (q^2 - q_{mod}^2)^2} \frac{\sin qx}{qx},$$

where $x = |\mathbf{x}|$. After evaluating this integral by contour integration and the residue theorem, we obtain the following result,

$$\begin{aligned} \langle \mathbf{P}(\mathbf{x}) \cdot \mathbf{P}(\mathbf{0}) \rangle &= \frac{k_B T}{2\pi \xi^{-2}} \frac{q_{mod}^5}{\tau_{mod}^0} e^{-q_{mod} r \sqrt{\frac{\sqrt{1+(q_{mod}\xi)^{-4}-1}}{2}}} \\ &\quad \times \sin \left(q_{mod} r \sqrt{\frac{\sqrt{1+(q_{mod}\xi)^{-4}+1}}{2}} \right) / (q_{mod} x). \end{aligned}$$

For large correlation lengths ($q_{mod} \xi \gg 1$), we obtain,

$$\langle \mathbf{P}(\mathbf{x}) \cdot \mathbf{P}(\mathbf{0}) \rangle \simeq \frac{k_B T}{2\pi \xi^{-2}} \frac{q_{mod}^5}{\tau_{mod}^0} e^{-x/(2q_{mod}\xi^2)} \sin(q_{mod} x) / (q_{mod} x),$$

which is the desired result. We note the calculation of the correlation function in the Gaussian approximation is identical to the one presented here except that one must replace $\tau \rightarrow r_0(T - T_0)$ in Eq. (S12) and define the correlation length as $q_{mod} \xi = (T_{mod}/(T - T_{mod}))^{1/4}$.

SUPPLEMENTARY NOTE 4. FITS TO EXPERIMENTS IN STO AND KTO

In this note, we describe our fits to the phonon spectra of STO and KTO. Our model has seven parameters r_0, T_0, u, c, a_t, v_t and h , which are given in Table I of the main text. For both materials, we have attempted fits for $f_s \geq f_{cr}$ and $0 \leq f_s < f_{cr}$.

Large couplings: $f_s \geq f_{cr}$ (i.e. $v_t \geq v_{cr}$)

STO: We take r_0, T_0 and u from Landau theory [S7]. Values for c, a_t , and v_t are available in Ref. [S8], however, they do not provide a good fit to the recent neutron scattering experiments of Ref. [S9]. We thus provide a new parametrization.

From the Supplementary Note 2, we have $a_t = \hbar^2 C_s / \rho$. We take $C_s = 1.24 \times 10^{11}$ N m⁻² from the observed low-temperature shear modulus and $\rho = 5.104 \times 10^3$ kg m⁻³ [S10]. To obtain c , we expand Eq. (S3a) to leading order in q , i.e., $\Omega_{\text{TO}}^2(\mathbf{q}) \simeq \tau + cq^2$ and fit it to the observed TO mode dispersion at 10 K [S9]. v_t and h were obtained by fitting $\tau_{\text{mod}}^{1/2}$ and q_{mod} to the zone center TO energy at low temperatures ($\simeq 1.70$ meV) [S11, S12] and to the wavevector minimum in the TA branch ($\simeq 0.024$ rlu) [S9], respectively.

KTO: To determine r_0, T_0 , and u , we first take the Landau limit of our model with a homogeneous polarization ($\mathbf{P}(\mathbf{x}) = \langle \mathbf{P} \rangle_{\text{MFT}}$) and $f_{\alpha\beta\gamma\lambda} = F_{\alpha\beta}(\mathbf{x}, \mathbf{x}') = 0$. We then fit r_0, T_0 , and u to the observed temperature and applied electric field dependence of the dielectric constant [S13, S14]. The values for c and a_t are known from neutron scattering experiments Ref. [S15]. v_t and h are obtained by fitting $\tau_{\text{mod}}^{1/2}$ and q_{mod} to the observed zone center TO energy at low temperatures ($\simeq 2.5$ meV) [S12, S15, S16] and the wavevector minimum in the TA branch ($\simeq 0.1$ rlu) [S17], respectively.

Small couplings: $0 \leq f_s < f_{cr}$ (i.e. $0 \leq v_t < v_{cr}$)

STO and KTO: We assume there is no long-range polar order in STO and KTO down to absolute zero, i.e., the energy gap of the zone-center TO phonon is finite at 0 K (see Eq. (S8)),

$$\tau = \Omega_{\text{TO}}^2(\mathbf{q} = 0) = -r_0 T_0 + (20u/3) \langle |\mathbf{P}|^2 \rangle > 0, \quad (\text{S13})$$

where $\langle |\mathbf{P}|^2 \rangle$ are the fluctuations of polarization calculated within the SCPA (see Supplementary Note 3). By taking r_0, T_0, u, c, a_t and h from the previous section and setting $\tau = 1.7$ meV (2.5 meV) for STO (KTO), we find that the inequality (S13) cannot be sat-

ified for $0 \leq v_t < v_{cr}$ in either material. We find the same result if we attempt to fit r_0, T_0 , and u while keeping the polarization physical, which we did by constraining r_0, T_0 , and u to produce the Landau value at 0K, i.e., $\langle \mathbf{P} \rangle_{\text{MFT}} = (\sqrt{2\epsilon_0} A \times 10^2) \sqrt{r_0 T_0 / (2u)} = 8.6 \mu\text{C}/\text{cm}^2$ ($2.3 \mu\text{C}/\text{cm}^2$) for STO (KTO), where ϵ_0 is the vacuum permittivity in units of $\text{C}^2 \text{N}^{-1} \text{m}^{-2}$, and $A = 194.4 \text{meV}$ (158.7meV) is a proportionality factor between the experimental zone-center TO frequency ($\Omega_{\text{TO}}^{\text{exp}}$) and the dielectric constant (ϵ^{exp}): $\Omega_{\text{TO}}^{\text{exp}} = A/\sqrt{\epsilon^{\text{exp}}}$ [S11]. $\sqrt{2\epsilon_0} A \times 10^2$ is a conversion factor from our model units to $\mu\text{C}/\text{cm}^2$.

By relaxing the polarization constraint and fitting r_0, T_0 and u to the observed zone-center TO mode, we find a fair agreement with experiments, as shown in Fig. S2. However, the resulting parametrization yields an unphysical $\langle \mathbf{P} \rangle_{\text{MFT}}$ (see Table S1).

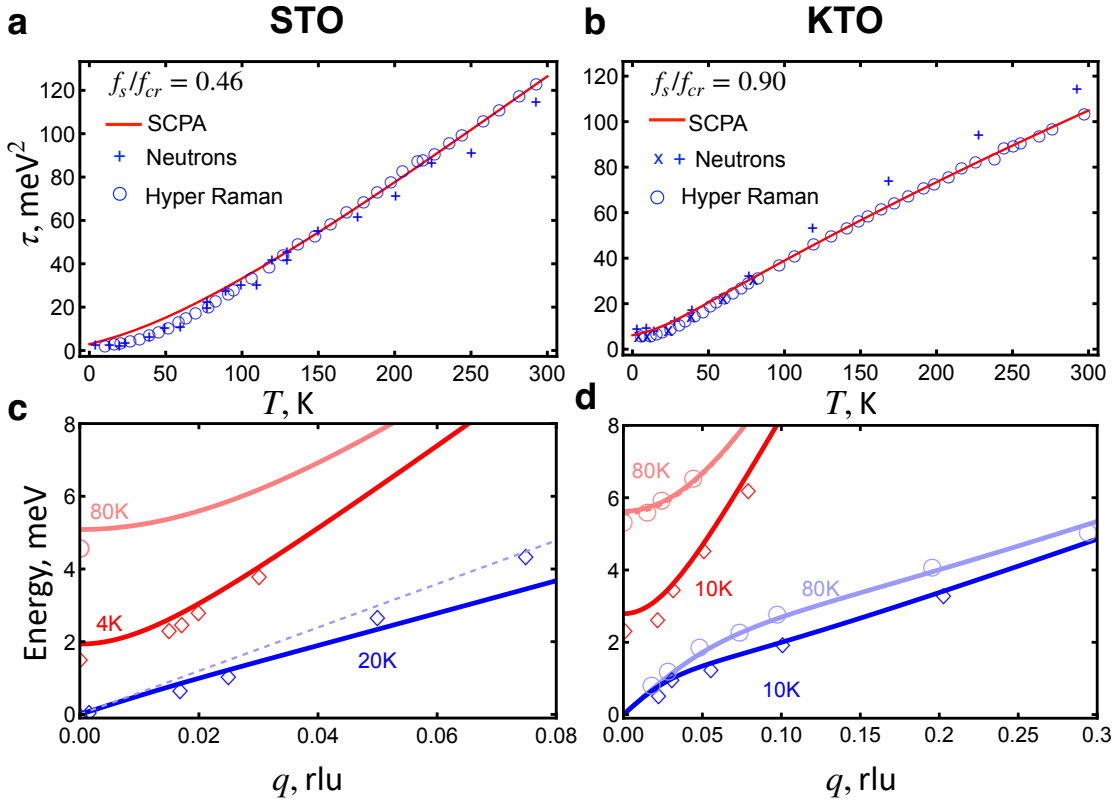


FIG. S2. (a),(b) Calculated temperature dependence of the zone center hybrid TO mode compared to neutron [S11, S15, S16] and hyper-Raman [S12] scattering experiments. (c),(d) Calculated dispersion of the hybrid TA and TO phonons (solid lines) compared to neutron scattering experiments (circles and diamonds) [S9, S15]. Dashed line in (d) is the bare linear TA dispersion for $f_s = 0$ with a sound velocity of 4800 m/s (as shown in Ref. [S9] for comparison). Model parameters are given in Table S1.

TABLE S1. Model parameters for small flexocouplings and no polarization constrain. For STO, we took c from Table I, v_t from Ref. [S8], and obtained r_0, T_0 and u by fitting Eq. (S8) to $\tau^{1/2} = 1.7, 6.7$ and 11.1 meV at $T = 0, 127,$ and 292 K, respectively, with $h = 0$. For KTO, we took c, a_t and v_t from Ref. [S15], and obtained r_0, T_0 and u by fitting Eq. (S8) to $\tau^{1/2} = 2.5, 7.1$ and 10.2 meV at $T = 0, 131,$ and 297 K, respectively, with $h = 0$. We could not fit the data for either material for $h > 0$.

	KTO	STO
r_0 [meV ² K ⁻¹]	0.16	0.20
T_0 [K]	100	473
u [10 ³ meV ³ rlu ⁻³]	0.12	1.29
c [10 ³ meV ² rlu ⁻²]	4.828 ^a	13.5
a_t [10 ³ meV ² rlu ⁻²]	1.553 ^a	2.739 ^b
v_t [10 ³ meV ² rlu ⁻²]	2.451 ^a	2.802 ^c
h [meV ⁴ rlu ⁻⁴]	0.0	0.0
$v_t/v_{cr} = f_s/f_{cr}$	0.90	0.50
$\langle \mathbf{P} \rangle_{\text{MFT}}$ [$\mu\text{C}/\text{cm}^2$]	0.02	0.02

^a From Ref. [S15].

^b From Ref. [S10].

^c From Ref. [S8].

-
- [S1] A. Aharony and M. E. Fisher, Critical behavior of magnets with dipolar interactions. i. renormalization group near four dimensions, *Phys. Rev. B* **8**, 3323 (1973).
- [S2] X. Oliver and C. Agelet de Saracibar, *Continuum Mechanics for Engineers. Theory and Problems* (2nd edition, 2017).
- [S3] H. Le Quang and Q.-C. He, The number and types of all possible rotational symmetries for flexoelectric tensors, *Proc. Royal Soc. A* **467**, 2369 (2011).
- [S4] B. A. Strukov and A. P. Levanyuk, *Ferroelectric Phenomena in Crystals: Physical Foundations* (Springer, 1998).
- [S5] P. M. Chaikin and T. C. Lubensky, *Principles of Condensed Matter Physics* (Cambridge University Press, 1995).
- [S6] E. Pytte, Theory of perovskite ferroelectrics, *Phys. Rev. B* **5**, 3758 (1972).
- [S7] K. M. Rabe, C. H. Ahn, and J.-M. Triscone, eds., *Physics of Ferroelectrics A Modern Perspective* (Springer-Verlag, 2007).
- [S8] V. G. Vaks, ed., *Introduction to the Microscopic Theory of Ferroelectrics* (Nakuna, 2007).

- [S9] B. Fauqué, P. Bourges, A. Subedi, K. Behnia, B. Baptiste, B. Roessli, T. Fennell, S. Raymond, and P. Steffens, Mesoscopic fluctuating domains in strontium titanate, *Phys. Rev. B* **106**, L140301 (2022).
- [S10] M. A. Carpenter, Elastic anomalies accompanying phase transitions in (Ca,Sr)TiO₃ perovskites: Part I. Landau theory and a calibration for SrTiO₃, *Am. Mineral* **92**, 309 (2007).
- [S11] Y. Yamada and G. Shirane, Neutron Scattering and Nature of the Soft Optical Phonon in SrTiO₃, *J. Phys. Soc. Jpn.* **26**, 396 (1969).
- [S12] H. Vogt, Refined treatment of the model of linearly coupled anharmonic oscillators and its application to the temperature dependence of the zone-center soft-mode frequencies of KTaO₃ and SrTiO₃, *Phys. Rev. B* **51**, 8046 (1995).
- [S13] H. Fujishita, S. Kitazawa, M. Saito, R. Ishisaka, H. Okamoto, and T. Yamaguchi, Quantum paraelectric states in SrTiO₃ and KTaO₃: Barrett model, Vendik model, and quantum criticality, *J. Phys. Soc. Jpn.* **85**, 074703 (2016).
- [S14] V. Skoromets, C. Kadlec, H. Němec, D. Fattakhova-Rohlfing, and P. Kužel, Tunable dielectric properties of KTaO₃ single crystals in the terahertz range, *J. Phys. D: Appl. Phys.* **49**, 065306 (2016).
- [S15] E. Farhi, A. K. Tagantsev, R. Currat, B. Hehlen, E. Courtens, and L. A. Boatner, Low energy phonon spectrum and its parameterization in pure KTaO₃ below 80 K, *Eur. Phys. J. B.* **15**, 615 (2000).
- [S16] G. Shirane, R. Nathans, and V. J. Minkiewicz, Temperature dependence of the soft ferroelectric mode in KTaO₃, *Phys. Rev.* **157**, 396 (1967).
- [S17] J. D. Axe, J. Harada, and G. Shirane, Anomalous acoustic dispersion in centrosymmetric crystals with soft optic phonons, *Phys. Rev. B* **1**, 1227 (1970).